Journal of Nuclear Materials 462 (2015) 85–90

Contents lists available at ScienceDirect

Journal of Nuclear Materials

journal homepage: www.elsevier.com/locate/jnucmat

Experimental determination of U diffusion in α-Zr

Jorge A. Gordillo [a], Rodolfo A. Perez [a,b,c,*], Manuel Iribarren [a,c], N. Di Lalla [b]

[a] Gerencia de Materiales, Comisión Nacional de Energía Atómica (CNEA), Avenida General Paz 1499, B1650KNA San Martín, Pcia. de Buenos Aires, Argentina
[b] Consejo Nacional de Investigaciones Científicas y Técnicas – CONICET, Avda. Rivadavia 1917, 1033 CABA, Argentina
[c] Instituto Sabato-UNSAM/CNEA, Avda. Gral. Paz 1499, 1650 San Martín, Argentina

HIGHLIGHTS

- Diffusion of U in α-Zr was measured for the first time.
- The used technique was α-spectrometry.
- An extended temperature range was studied 763–1123 K.
- A downward curvature in the Arrhenius plot was observed.
- The non-Arrhenius behaviour is similar to self-diffusion one.

ARTICLE INFO

Article history:
Received 28 November 2014
Accepted 17 March 2015
Available online 21 March 2015

ABSTRACT

U bulk diffusion in α-Zr was measured by mean α-spectrometry in the temperature range 763–1123 K (540–850 °C). A deviation from the Arrhenius law consistent in a downward curvature was observed; such anomaly is similar to the self and hetero substitutional diffusion previously measured in α-Zr matrix.

The measurements are compatible with the existences of migrating Fe–vacancy complex that could be competitive with a simplest single vacancy mechanism for substitutional diffusers. The possibility that this could be the reason for the non Arrhenius behaviour is discussed.

1. Introduction

The present work is part of two larger and systematic investigations, on one hand on U diffusion at infinite dilution in metals and in the other hand of substitutional diffusers in α-Zr with particular emphasis in those of interest in the nuclear industry.

The interest on the subject lies in the fact that the available U diffusion coefficients at infinite dilution in the literature are scarce, mostly measured in the 60's and 70's Cf Ref. [1] for a list of the measurements performed up to 1990. Besides, a quick (probably not exhaustive) literature search (e.g. Ref. [2] and the Scopus data base) suggests there are no measurements of diffusion at infinite dilution in pure metals newer than the mentioned ones.

Regarding U diffusion in Zr at infinity dilution, the available data is restricted to the bcc β phase [3] measured by direct sectioning in the temperature range 1223–1773 K. Extending the scope to interdiffusion in U–Zr solid solutions, a couple of works [4,5] were reported. In particular in [4] Zr concentration goes from 0.1 to 0.95 atomic fraction where chemical diffusion coefficient $\widetilde{\boldsymbol{D}}$ is measured in the temperature range 973–1123 K in the (γ-U, β-Zr) phase, where neither intrinsic, nor infinite dilution diffusion coefficients were obtained.

Up to our knowledge, there are not data for U diffusion at infinite dilution in the low temperature hcp α phase reported at present.

In order to extend diffusion measurements to the hcp α phase, our first task was to adapt the α spectroscopy reliable technique, to the determination U diffusion profiles, in a sub-micrometric depth scale [6]; in this way and taking into account the depth resolution of the technique reported in this work, we were able to apply α spectroscopy and perform non destructive measurements in pure α-Zr samples, down the α/β transition temperature ($T_{\alpha/\beta}$ = 1136 K) to lowest ones in the frame of reasonable annealing times (around 10^7 s).

On the other hand, it is well established that α-Zr self-diffusion do not follow the Arrhenius law, a downward curvature is observed once a large enough temperature range is studied [7].

Since the early 70s there have been reports in the literature that some metallic elements such as Fe, Co, and Ni dissolved in hexagonal Zr behave as ultra-fast diffusers [8–10]; namely, their diffusion

* Corresponding author at: Gerencia de Materiales, Comisión Nacional de Energía Atómica (CNEA), Avenida General Paz 1499, B1650KNA San Martín, Pcia. de Buenos Aires, Argentina.
E-mail address: rodperez@cnea.gov.ar (R.A. Perez).

http://dx.doi.org/10.1016/j.jnucmat.2015.03.037
0022-3115/

coefficients, close to the hcp/bcc transformation are over 10^6 times higher than the host self-diffusion one. The observations referred mainly to well annealed, single or large grain polycrystalline samples, thus essentially ruling out possible extrinsic effects. Such huge figures were interpreted as the outcome of an interstitial-like diffusion mechanism, idea that was thought to apply also to other earlier studied systems, such as Au into Pb [11]. Further experiments followed through the 80s and 90s, becoming clear that reliable extraction of the diffusion parameters, i.e., activation energy and pre-exponential factor, was an especially difficult task. Tracer hold up at the surface, back diffusion, general non-Arrhenius behavior of the profiles, were rather common issues, demanding non-standard corrective procedures at both, experimental and data analysis stages. Sample purity is an added concern to the list, as it was evident that a sort of defect complexing impacted solute diffusion at low temperatures. These problems plagued dramatically the Zr host, where all the solutes named show a downwards curvature in the (Arrhenius) plots of ln D versus T^{-1}. Such a result, coupled to the limited extent of the hcp phase in the high temperature region, renders the estimation of diffusion parameters rather uncertain.

When sub-micrometric techniques (essentially Ion Beam Sputtering: IBS, Rutherford Backscattering Spectrometry: RBS and Heavy Ion RBS: HIRBS) were available and the temperature range in the hcp diffusion studies was extended, similar deviations from the classical Arrhenius behaviour were observed in substitutional diffuser in α-Zr [12–14] in all cases, including the interdiffusion measurements in Ref. [4], a break at around 1000 K is observed which can be interpreted either as a downward curvature [7] or as two regions, where the one below 1000 K could reflect the formation of not identified solute atom complexes [10]. Whether that behaviour is an intrinsic effect or the consequence of the interaction between ultrafast impurities and the diffusing atom is an open discussion topic in the literature (see for example [15] and references therein). In this frame a similar behaviour could be expected for U diffusion in the α-Zr matrix.

2. Experimental method

The measurements were performed in high purity (99.97%) discs of Zr of about 12 mm in diameter and 3 mm thickness. Table 1 reports a complete list of the impurity content. Let's remarks the Fe content of 150 μg/g.

The samples were mechanically polished and subjected to an annealing cycle in order to increase their grain size: 1 h at 1473 K followed by 20 days at 1133 K, in highly pure argon atmosphere. This procedure led to samples with at most 3–4 large grains. A micrography showing the grain size in a typical sample, revealed by thermal etching, is shown in Fig. 1. In the upper grain, the small black dots and stripes observed are product of poor polishing. Subsequently the samples were mechanically and chemically polished again in order to obtain very flat surfaces. After that a new annealing for 1 day at 1123 K was performed in order to release stresses originated during the process.

Diffusion pairs were obtained by evaporation of depleted U, 99.97% purity, onto the sample surface, by heating a tungsten filament in a vacuum better than 10^{-6} torr. The α-spectrum taken after the deposition and before diffusion annealing (full line in Fig. 2) shows, thorough the analysis presented in Section 3, that the U layer deposited is less than 9 nm.

The diffusion anneals were performed under dynamic vacuum, 2×10^{-6} torr, when the total annealing time was shorter than 2×10^5 s, or in sealed quartz tubes under high purity argon for longer times. To prevent reactions between Zr and quartz, the samples were wrapped into Ta foils. The diffusion temperatures were controlled within ±1 K with a Pt–PtRd S type thermocouple.

A silicon base p–n junction surface barrier detector (Canberra PD 150-16-100-AM) was used in order to measure the α spectra, with an active surface of 150 mm^2 and an energy nominal resolution of 16 keV. As neither the detector nor the samples are points, the solid angle subtended between them is not unique. In order to test their influence in the peak width we change the sample-detector distance between 2 and 10 cm, inside the vacuum

Fig. 1. Optical micrography (5×) corresponding to a typical α-Zr sample after growth and stabilization annealing. A few large grain sizes were obtained.

Table 1
α-Zr samples impurity content.

Impurity	Content (μg/g)
Al	<10
Cd	<0.5
Co	<10
Cr	<10
Cu	<10
Fe	150
Hf	64
Mn	<10
Mo	<10
Ni	<10
Pb	<20
Si	<30
Sn	<30
Ti	<10
V	<10
C	29
N	11
O	<50

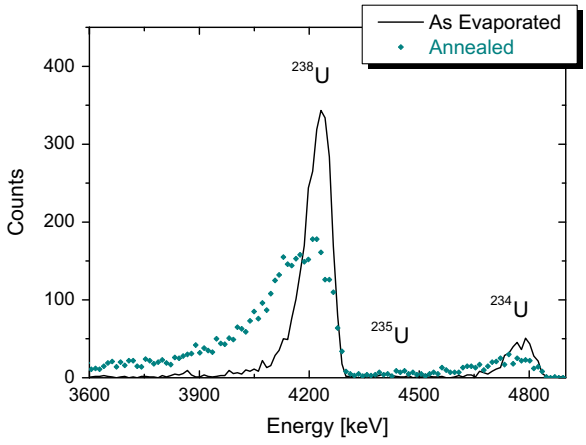

Fig. 2. α spectra, before and after diffusion annealing.

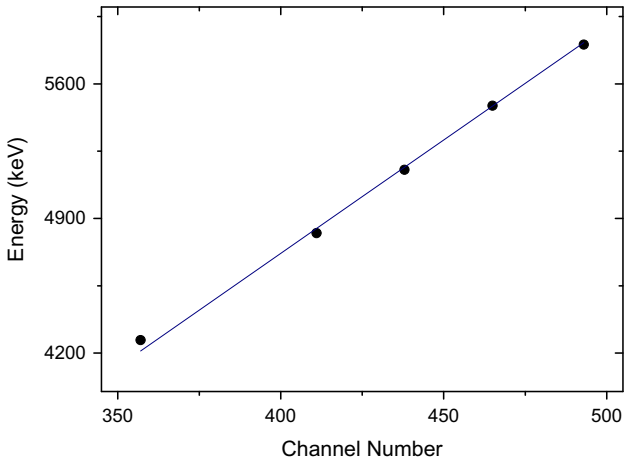

Fig. 3. α spectra energy calibration.

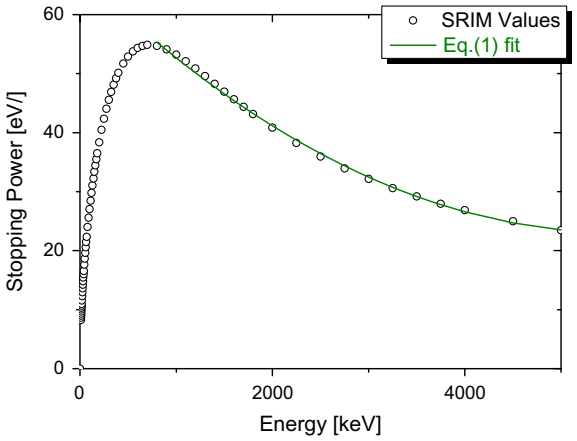

Fig. 4. α particle stopping power dependence with energy in Zr matrix.

chamber. Of course, an increment in the distance implies an increment in the acquisition time, but not significant variation in the peak width was observed. Consequently, in order to minimize the acquisition time, a distance of 2 cm between sample and detector was chosen. Typical acquisition times were between 20 and 40 h.

Calibration in energy was made using three α peaks from a ^{241}Am standard source, one from a ^{233}U standard source and the last one is the ^{238}U peak. Calibration curve is given in Fig. 3.

The (as evaporated) initial spectra was fitted with a gaussian function whose width is given by the convolution of the effect of the α emission depth across the U deposit, the electronic noise, and the difference in the particle path due to the solid angle subtended between the sample and the active surface of the detector. Other noise contributions, like straggling, could be neglected. In this particular case, the initial width was 45 keV.

3. Data analysis

A carefully detailed description of the α spectrometry as applied to measure the U diffusion coefficient in metals is given in Ref. [6]. We now proceed to apply it to the α-Zr case.

Fig. 2 (full line) shows the α particles spectra measured after U deposition, before the diffusion annealings; we focus the analysis on the particles emitted by the ^{238}U isotope. After annealing, there is a spectrum broadening towards low energies (Fig. 2 doted line) given by the increase in the emitter distance to the surface due to diffusion, entailing larger energy losses.

This energy loss is given by the stopping power (dE/dx) as was defined, for instance, in Ref. [16]; it was calculated by the subroutine "stopping range" from the program SRIM 2008 [17] for α particle moving in Zr between 10 keV and 5 MeV, with an error estimation lower than 3%.

The α-particle stopping power dependence with the energy for this particular case is shown in Fig. 4. The solid line is a data parabolic fit valid between 800 keV and 5 MeV:

$$dE/dx(E) = a + b \cdot E + c \cdot E^2 \tag{1}$$

being $a = 66.9913848$ eV Å^{-1}, $b = -1.5731277 \times 10^{-5}$ Å^{-1} and $c = 1.4080616 \times 10^{-12}$ eV^{-1} Å^{-1}.

Then, when the α-particle is emitted by a ^{238}U atom from a distance x to the surface:

$$x = -\int_{E_0}^{E_d} \frac{dE}{dE/dx} = -\int_{E_0}^{E_d} \frac{dE}{a + bE + cE^2} \tag{2}$$

where E_0 is the energy of the α-particle when emitted (4.267 MeV) and E_d is the detected energy when arriving at the sample surface.

Analytic integration of expression (2) is straightforward, giving a relationship between the U depth and the detected energy:

$$x(E_d) = \frac{1}{\sqrt{ac - (b/2)^2}} \left[\arctan\left(\frac{cE_0 + b/2}{\sqrt{ac - (b/2)^2}} \right) - \arctan\left(\frac{cE_d + b/2}{\sqrt{ac - (b/2)^2}} \right) \right] \tag{3}$$

when $(b^2 - 4ac) < 0$ as in the present case.

Eq. (3) shows a bijective correspondence between energy lost and depth, and consequently, with the spectrum channel number. On the other hand, the amount of U at each depth is directly related to the amount of counts cumulated in that channel.

So, all the information in order to obtain a typical diffusion profile, concentration versus depth is now available.

4. Results and discussion

Given the initial thickness of the as deposited U, a Gaussian shape solution to Fick's law is proposed:

$$C(x) = \frac{C_0}{\sqrt{\pi D(t + t_0)}} \exp\left(\frac{-x^2}{4D(t + t_0)} \right) \tag{4}$$

where C is the U concentration at depth x, C_0 is the initial amount of U per unit of area at the surface, D is the diffusion coefficient at a given temperature, t is the annealing time and t_0 is a fitting parameter coming from the initial profile (before the diffusion annealing) used in order to perform a deconvolution to its initial width as described in [6].

Typical diffusion profiles ln [$C(x)$] versus x^2 were built, with the algorithm described in Section 3. They are shown, for each temperature studied, in Fig. 5a and b. In all cases straight lines were obtained, that means all the deposited U diffuses in solid solution in the α-Zr matrix, thus Eq. (4) is satisfied as expected. Diffusion coefficients are obtained from:

$$D = \frac{s - s_0}{4ts s_0} \tag{5}$$

where s is the slope of the diffusion profile and s_0 is the one of the as-evaporated initial profile.

A complete list of temperatures, diffusion annealing times and D values at each temperature is given in Table 2.

Fig. 6 is an Arrhenius plot [ln (D) versus T^{-1}] for all those D values; a non Arrhenius behaviour in the U diffusion results is evident, but less pronounced that the one observed in the α-Zr

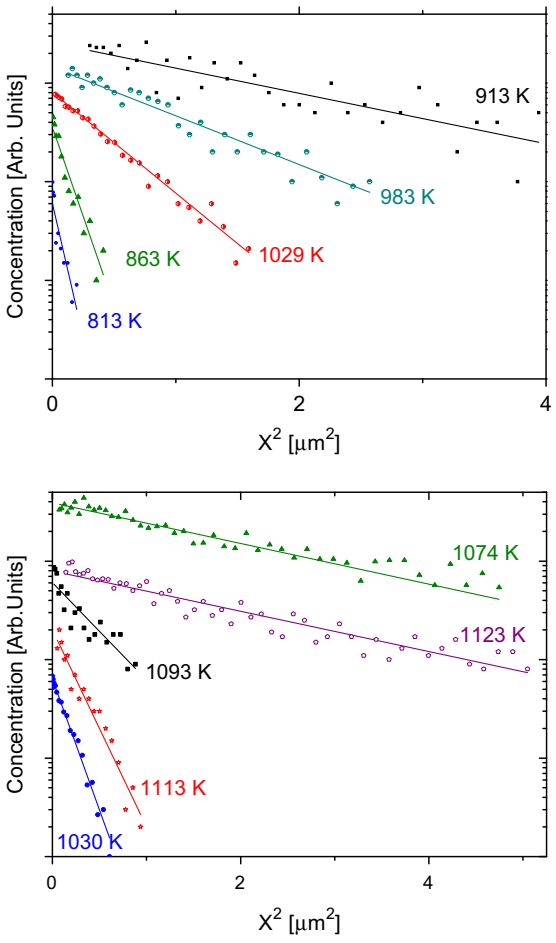

Fig. 5. (a and b) U diffusion profiles in α-Zr for all measured temperatures.

Table 2
D values measured at different temperatures.

Temperature (K)	t (10^4 s)	D ($m^2\,s^{-1}$)
1123	1.08	$(1.4 \pm 0.4) \times 10^{-17}$
1113	0.36	$(1.0 \pm 0.3) \times 10^{-17}$
1093	1.44	$(6.3 \pm 0.6) \times 10^{-18}$
1074	8.28	$(4.5 \pm 0.5) \times 10^{-18}$
1030	8.64	$(1.4 \pm 0.3) \times 10^{-18}$
1029	21.6	$(1.1 \pm 0.4) \times 10^{-18}$
983	86.4	$(2.5 \pm 0.3) \times 10^{-19}$
913	829.44	$(4.8 \pm 0.8) \times 10^{-20}$
863	1071.36	$(1.5 \pm 0.3) \times 10^{-21}$
813	2341.44	$(1.0 \pm 0.3) \times 10^{-22}$

self-diffusion [7]. It can be thought either as a downward curvature or as a break in two different regions, above and below 1000 K.

This kind of non Arrhenius behaviour was observed in most diffusers studies in α-Zr when the temperature range is large enough (see [15] and references therein) and seems to be related to the amount of ultra-fast impurities, in particular Fe, present in the α-Zr matrix, even though an intrinsic effect cannot be disregarded.

In Fig. 6 U diffusion coefficients are in an Arrhenius plot together with the α-Zr self-diffusion measured in two matrices with different Fe contents: the purest samples (around 20 μg/g of Fe) from [7] and samples with a higher amount of Fe (160 μg/g) [18]; this last amount is similar to the impurity content in the present work samples (150 μg/g). An increment in the self-diffusion values due to the increase on the ultra-fast Fe impurity is evident. If we compare U diffusion in α-Zr from this work, it is clear that they are closer to the self-diffusion data measured in least pure

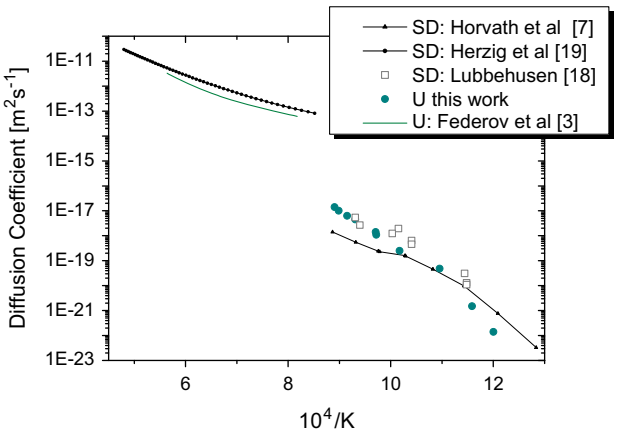

Fig. 6. Self-diffusion and U diffusion in both α-Zr and β-Zr matrices.

α-Zr samples [18] than the ones measured in the purest ones [7]. This behaviour is congruent with the hypothesis that the presence of Fe increases the diffusion process.

Also in the Arrhenius plot in Fig. 6, U diffusion in β-Zr phase [3] and β-Zr self diffusion [19] are shown together. In this case, the reason for the curvature observed in the β-phase in both diffusers is well established as a phonon softening of the mode LA 2/3 ⟨1 1 1⟩ effect, an intrinsic characteristic of bcc structures that diminish the energy required to move a vacancy when the temperature goes down until it reaches $T_{\alpha/\beta}$ (see for instance [20]).

U diffusion in the β-phase follows the self-diffusion behaviour: U diffusion coefficients D values are close but systematically lower and the curvature in the Arrhenius plot is similar. A vacancy mechanism ruling the U diffusion process in β-Zr is consistent with this behaviour.

Below $T_{\alpha/\beta}$ diffusion coefficients for both, α-Zr self-diffusion [7,18] and U diffusion (this work) drop between 3 and 4 orders of magnitude, mainly due to the phase transition from an open bcc structure to a close hcp structure. Again *D* values are similar in both cases and the U ones are almost equal or lower than the self-diffusion ones [18] when they are measured in α-Zr matrixes with similar Fe content.

Nonetheless, the origin of the deviation from the Arrhenius law in the α-phase is not so well established as in the β-phase. It seems to be clear that a similar, although not well known, mechanism could be the responsible in both cases.

As we pointed out, the presence of the ultra-fast impurity Fe seems to be the key in order to understand the origin of this anomalous behaviour. Nevertheless up to day a complete explanation is not given in the literature. This is essentially an experimental work nevertheless, in what follows we are going to enumerate a number of elements in order to begin to understand the phenomena.

The first step consists into establish the existence of a complex vacancy–Fe mechanism with lower formation and migration energies than a single vacancy in order to mediate in the self-diffusion enhancement. If it exists, any substitutional element in the α-Zr matrix, like U, could migrate via such complex.

The second and more difficult step, is to find a reason on why one or several of such vacancy–Fe complex could be activated or deactivated at different temperatures in order to explain the apart from the Arrhenius law.

A possible Fe–vacancy complex, as the one discussed above was recently presented in [21]. According to *ab initio* calculations, the Fe atoms present as impurities in α-Zr lattice are stables in a set of quasi-degenerated configuration: octahedral position is the most stable one but the so called off-site configuration has an

energy formation only 0.36 eV higher. In the off-site configuration the Fe atom is slightly displaced from the lattice node towards the octahedral position, whereas four nearest neighbour Zr atoms move closer to the Fe atom. The interatomic distances decrease to around 2.5 Å from the 3.13 Å nearest neighbour distance in the perfect α-Zr lattice. Such distance and configuration are similar to the interatomic distances and configuration in ZrFe intermetallic compounds: Zr_3Fe or Zr_2Fe [22]. Also in the octahedral position the equilibrium distance between Fe and a nearest neighbour Zr is 2.43 Å. For both configurations, off-site and octahedral, there is a strong interaction among the involved species valence electrons.

The off-site Fe presence produces both a decrease in the vacancy formation energy and a distortion of the lattice, with Zr atoms displaced from their lattice nodes towards the Fe site. In order to explain the diffusion enhancement a mechanism involving the movement of the complex Fe–vacancy as a whole was calculated obtaining an energy cost 0.4 eV lower than the single vacancy mechanism.

As the off-site Fe with a nearest neighbour vacancy can dissociates into an octahedral Fe plus a second neighbour vacancy, an effective three-dimensional Zr migration can result from the displacement of an off-site Fe into another off-site position, passing through an octahedral position with a second neighbour vacancy. The activation energy associated to this process is almost 0.4 eV smaller than the single vacancy exchange. A detailed displacement description and involved energies calculation is given in [21].

The first step, to found a possible mediating mechanism for the enhancement in the diffusion processes due to Fe presence, was fulfilled. Unfortunately, to introduce temperature in *ab initio* calculations is not an easy task, so the evolution with temperature, the cross interaction with single vacancy mechanism and/or another kind of Fe–vacancy complex that could explain the curvature in the Arrhenius plot is not determined yet.

Another characteristic shared among diffusers in α-Zr is that when their diffusivity is studied in α-Ti the Arrhenius law is observed at all temperature. When U diffusion was also studied in our laboratory using the same α-spectroscopy technique [23], a straight Arrhenius plot is obtained with a well defined activation energy Q and pre-exponential factor D_0 characterizing the diffusion process.

α-Ti is in the same column IV-B in the periodic table than α-Zr, and they share several thermodynamic, chemical and mechanical characteristics. The first works trying to explain the non Arrhenius behaviour in α-Zr (in particular [24]) were based in the idea that the break at around 1000 K was related with the precipitation of Fe in solution and consequently claim that the same break should be present in α-Ti matrix at lower temperatures given the higher Fe solubility. Nevertheless, when the Co diffusion in α-Ti was measured at low temperatures [25], between 823 and 619 K (600 and 346 °C) not curvature was observed and the results align perfectly well with previous data measured at higher temperature, from $T_{\alpha/\beta}$ to 823 K [26] with the same diffusion parameters.

This behaviour: downward curvature for diffusion in α-Zr and straight Arrhenius plot for α-Ti, is observed for all diffusers, including self diffusion, when they were measured in both matrices, in an extended temperature range (see [15] and references therein). Again, our measurements for U diffusion are in line with those previous results.

A more elaborated mechanism than the simple Fe precipitation responsible for non Arrhenius ultra-fast impurity diffusion was recently given by means of *ab initio* calculations in [27]. Diffusion behaviour of ultra-fast diffusers: Fe, Co and Ni in both α-Ti and α-Zr matrices were modelled. The migrating specie may adopt any of three states: (1) a highly mobile interstitial, (2) (relatively) immobile quasi-substitutional and (3) (relatively) immobile trapped at impurities dumbbell configuration. A dissociative mechanism was postulated and so the explanation for the differences between both matrices relies on the relationship among binding energies of these states in each matrix. Even though extrapolation of that model to substitutional diffusers like U is not straightforward, our experimental results go into this direction.

Finally let's say a word regarding the determination of activation energy Q and pre-exponential factor D_0 in non Arrhenius systems.

In cases where the superposed mechanisms responsible for non Arrhenius behaviour are well established, determination of Q and D_0 as the slope of the Arrhenius curve at a given temperature could be useful. This is the case, for instance, in fcc metals where at low temperature a single vacancy mechanism is dominant, then the slope at this low temperatures gives the activation energy associated to vacancy formation and migration in the lattice, whereas at temperatures close to the melting point T_m, divacancies are dominant and now the slope close to T_m is related to their formation and migration energies.

Extrapolate this procedure to any non Arrhenius system is not always correct. Let's analyze what happen when Q depends with the temperature, as is the case for diffusion in ferromagnetic α-Fe.

Example. Activation energy for diffusion in ferromagnetic α-Fe

The ferromagnetic spins alignment in α-Fe results in a dependence of Q with the temperature given by (see for instance [28]):

$$Q_f(T) = Q_p(1 + \alpha\, S(T)) \tag{6}$$

where Q_p is the activation energy in the paramagnetic region, α is an adimensional constant and $S(T)$ is the ratio of the spontaneous magnetization at temperature T to the one at 0 K (reduced magnetization).

The Arrhenius curve slope is defined by:

$$\text{slope} = \frac{\partial[\ln(D/D_0)]}{\partial 1/T} \tag{7}$$

of course, in an Arrhenius systems (7) is directly $-Q/K$; but for ferromagnetic α-Fe is:

$$-K * \text{slope} = Q_p(1 + \alpha\, S(T)) + \frac{\alpha\, Q_p}{T}\frac{\partial S(T)}{\partial 1/T} = Q_f(T) + \frac{\alpha\, Q_p}{T}\frac{\partial S(T)}{\partial 1/T} \tag{8}$$

Then the activation energy in α-Fe ferromagnetic diffusion at a given a temperature is (6) and the slope of the Arrhenius curve at the same temperature is (8). The difference between both is a temperature depending factor.

In fact, it is well established, both experimental and theoretically [28,29], that the ferromagnetic alignment induce a stiffness in the lattice and consequently an increment in the activation energy ($\alpha\, S(T) > 0$), whereas the slope in the Arrhenius curve, for instance for Nb diffusion in α-Fe [28], diminish at low temperatures with respect to the one in the paramagnetic region (the derivative of $S(T) < 0$).

Summarizing, in the present work we can calculate the diffusion parameters above and below 1000 K, which is done it in the next paragraph, but without knowing the mechanism or mechanisms responsible for the curvature, their meaning is not straightforward.

If we consider only the first 7 D values obtained at temperatures closer to $T_{\alpha/\beta}$ the diffusion parameters are $Q = 259.2$ kJ/mol and $D_0 = 1.6 \times 10^{-5}$ m^2 s^{-1}. Considering only the lower temperature 3 Ds now $Q = 358.5$ kJ/mol and $D_0 = 12$ m^2 s^{-1}. Considering the lower 4 Ds the parameters change to $Q = 305.3$ kJ/mol and $D_0 = 6.3 \times 10^{-3}$ m^2 s^{-1}.

We can change the set of data involved in each calculation with a wide scatter in the diffusion parameters so, as we pointed out, whether or not they are the actual values at each temperature it is not clear.

5. Conclusions

U diffusion in α-Zr in the temperature range 813–1123 K was determined using α spectrometry, a sub-micrometric technique capable to extend the temperature range of measurements below half the melting point.

Arrhenius plot for U diffusion in α-Zr shows a downward curvature which is analogue to the ones observed in self-diffusion and most of the diffusers studied in this matrix.

The existence of a Fe–vacancy complex with activation energy lower than the single vacancy one, as previously calculated by *ab initio* methods, and candidate to be responsible for the influence of ultra-fast impurities, like Fe, in the diffusion in α-Zr is compatible with our results.

Acknowledgment

This work was partially supported by the Consejo Nacional de Investigaciones Científicas y Técnicas CONICET PIP 0804/10.

References

[1] Landolft-Börnstein, Diffusion in Solid Metals and Alloys, Springer-Verlag, Berlin, Heidelberg, 1990 (Compiled by H. Mehrer).
[2] G. Neumann, C. Tujin, Self-diffusion and Impurity Diffusion in Pure Metals: Handbook of Experimental Data, Pergamont Materials Series 14, Elsevier Ltd, Amsterdam, Netherlands, 2009.
[3] G.B. Federov, E.A. Smirnov, F.I. Zhomov, F.I. Gusev, S.A. Paraev, Metall. Metalloved. Chist. Met. 9 (1971) 30.
[4] T. Ogata et al., J. Nucl. Mater. 232 (1996) 125–130.
[5] Y. Adda, J. Philibert, H. Faraggi, Rev. Metall. 54 (1957) 597.
[6] R.A. Pérez, J. Gordillo, N. Di Lalla, Measurements 45 (7) (2012) 1836.
[7] J. Horváth, F. Dyment, H. Mehrer, J. Nucl. Mater. 126 (1984) 206.
[8] G.M. Hood, R.J. Schultz, Philos. Mag. 26 (1972) 329.
[9] G.M. Hood, R.J. Schultz, Phys. Rev. B 11 (1975) 3780.
[10] G.V. Kidson, Philos. Mag. 44 (1981) 341.
[11] W.K. Warburton, Phys. Rev. B 11 (1975) 4945.
[12] G.M. Hood, H. Zou, R.J. Schultz, J.A. Roy, J.A. Jackman, J. Nucl. Mater. 189 (2) (1992) 226.
[13] R.A. Pérez, F. Dyment, Diffus. Solids Liquids 2 (2005) 539.
[14] R.A. Pérez, F. Dyment, Appl. Phys. A 68 (1999) 667.
[15] R.A. Pérez, H. Nakajima, F. Dyment, Mater. Trans. 44 (2003) 2.
[16] C.W.K. Chu, Rutherford Backscattering Spectrometry ASM Handbook, vol. 10, Materials Characterization, ASM International, Member/Customer Service Center, Materials Park, OH 44073–0002, USA, 1986.
[17] J.F. Ziegler, J.P. Biersack, M.D. Ziegler, SRIM – The Stopping and Range of Ions in Matter, 2008.
[18] M. Lübbehusen, K. Vieregge, G.M. Hood, H. Mehrer, Chr. Herzig, J. Nucl. Mater. 182 (1991) 164.
[19] Ch. Herzig, H. Eckseler, Z. Metallkd 70 (1979) 215.
[20] Ch. Herzig, Defect Diffus. Forum 95–98 (1993) 203.
[21] R.C. Pasianot, R.A. Pérez, V.P. Ramunni, M. Weissmann, J. Nucl. Mater. 392 (2009) 100.
[22] J.L.C. Daams, P. Villars, J.H.N. van Vucht, Atlas of Crystal Structure Types, vol. 3, ASM International, 1991.
[23] R.A. Pérez, J.A. Gordillo, N. Di Lalla, Philos. Mag. A 93 (17) (2013) 2219.
[24] G.M. Hood, J. Nucl. Mater. 135 (1985) 292.
[25] R.A. Pérez, F. Dyment, Philos. Mag A 71 (5) (1995) 965.
[26] H. Nakajima, M. Koiwa, Y. Minonishi, S. Ono, Trans. Japan Inst. Metals 24 (1983) 655.
[27] R.C. Pasianot, R.A. Pérez, Physica B 407 (2012) 3298.
[28] R.A. Pérez, Appl. Phys. A 92 (2) (2008) 325.
[29] R.A. Pérez, D.N. Torres, F. Dyment, M. Weissman, Defect Diffus. Forum 337–340 (2005) 462.